

Article

# Controls on Land Surface Temperature in Deserts of Southern California Derived from MODIS Satellite Time Series Analysis, 2000 to 2018

Christopher Potter <sup>1,\*</sup> and Dana Coppernoll-Houston <sup>1,2</sup>

<sup>1</sup> NASA Ames Research Center, Moffett Field, CA 94035, USA

<sup>2</sup> Thomas Jefferson High School, Federal Way, Auburn, WA 98001, USA; Dana.Coppernoll@nasa.gov

\* Correspondence: chris.potter@nasa.gov; Tel.: +1-650-604-6164

Received: 3 December 2018; Accepted: 1 February 2019; Published: 11 February 2019

**Abstract:** The land surface temperature (LST) in arid regions is a primary controller of many ecological processes. Consequently, we have developed a framework for detection of LST change on a regional scale using data sets covering all deserts of southern California from the Moderate-Resolution Imaging Spectroradiometer (MODIS) satellite sensor. The Breaks for Additive Season and Trend (BFAST) methodology was applied to MODIS 1-km monthly LST data from the years 2000 to 2018 to estimate significant time series shifts (breakpoints) and gradual trends. Area-wide results showed five times more positive LST breakpoints (abrupt temperature warming events) than negative (surface cooling) breakpoints. Cross-correlations with high rainfall periods around Mojave dry lake playas, and comparison with timing of wildfire burns for breakpoint patterns, showed that abrupt shifts in LST had the strongest response to these controllers. We detected negative LST (abrupt cooling) breakpoints as consistently associated with the construction of new solar energy facilities. Over the majority of the study area, BFAST results showed warming LST trends between the years 2000 and 2018. The western-most margins of the study area showed consistent widespread warming trends, whereas the eastern portions of the Mojave and Lower Colorado Deserts showed a mix of positive and neutral LST trends. Long-term cooling LST trends were detected only in some of the largest dry lake formations in the Antelope Valley, Death Valley, and Bristol, Cadiz, and Danby playas.

**Keywords:** surface temperature; MODIS; thermal infra-red; Mojave Desert; Lower Colorado Desert; precipitation

---

## 1. Introduction

Long-term changes in land surface temperature can influence interacting ecological and geochemical processes in desert landscapes, including plant cover distributions, activity of wildlife populations, soil microbial activity, evapotranspiration, and trace gas emissions [1]. Slope, vegetative cover, water content, bulk density, and a host of other factors affect how much heat from solar irradiance a soil can absorb or re-emit [2].

Land cover disturbance from renewable energy development in arid ecosystems is receiving increasing attention due to potential impacts on protected area conservation, endangered species, and air quality [3]. Over the past decade, new solar energy facilities have been built in parts of southern California's Mojave and Lower Colorado Deserts under the Desert Renewable Energy Conservation Plan (DRECP). The DRECP covers parts of seven California counties: Imperial, Inyo, Kern, Los Angeles, Riverside, San Bernardino, and San Diego. Approximately 91,000 km<sup>2</sup> of federal and non-federal California desert land form part of the DRECP area.

A major purpose of the DRECP is to “provide effective protection and conservation of desert ecosystems while allowing for the appropriate development of renewable energy projects” [4]. Development Focus Areas (DFAs) under the DRECP are located on public lands under the Bureau of Land Management, who thus have the responsibility of maintaining this balance between renewable energy and ecosystem preservation. DFAs have been specially designated areas approved by the DRECP where construction of renewable energy sites, for the most part solar energy, has been fast-tracked.

Satellite remote sensing provides a practical mean to monitor day-to-day temperature fluctuations across large regions. Previous research by Li et. al. [5] (2008) showed a correlation between air temperature and land surface temperature (LST) from the Advanced Very High Resolution Radiometer (AVHRR) instrument on the National Oceanic and Atmospheric Administration (NOAA) polar-orbiting satellites, with  $R^2$  values of 0.54, 0.42, and 0.62 over three years. Despite differences in air temperature and LST values, it was shown that a linear model can be developed to enhance accuracy. Quan et al. [6] reported that Moderate-Resolution Imaging Spectroradiometer (MODIS) LST around Beijing, China had decreasing trends from 2000 to 2012 that were more pronounced over croplands than over urban lands. Zhan et al. [7] developed methods to disaggregate LST by the parameters of various temperature cycle models. Coppernoll-Houston and Potter [8] reported that Landsat LST was closely correlated with site measurements of air and surface temperatures in solar energy development zones of southern California, allowing inter-conversion of satellite data with ground-based measurements for use in desert ecosystem change studies.

For this study, we used an 18-year LST time series at 1-km resolution from Collection 6 of the Moderate-Resolution Imaging Spectroradiometer (MODIS) satellite with the Breaks for Additive Season and Trend (BFAST) method [9] to detect significant structural changes in ground temperatures over time for deserts of southern California. Abrupt shifts, or “breakpoints,” may adversely affect ecosystem health because wildlife populations may not adapt quickly to new conditions. A positive (abrupt warming) breakpoint in LST may be indicative of either rapid drainage and drying of a large area, or the sudden loss of all live green vegetation due to burning or clearing, either of which raises surface temperatures abruptly. A negative (abrupt cooling) breakpoint in LST may be indicative of rapid filling of a large area with ponded surface water that drops the surface temperatures suddenly. A primary objective of the study was to assess the influence of solar energy development sites in parts of the Mojave and Lower Colorado Deserts on LST patterns, and to thereby develop a reproducible framework for ecological change detection.

## 2. Study Area

The 122,160 km<sup>2</sup> study area for this time series analysis of LST covered the DRECP boundary region in California (Figure 1). Low annual rainfall (50–300 mm) and high temperatures (exceeding 45 °C in the summer) make this area one of the most arid in North America [10]. The main perennial vegetation cover types are creosote bush (*Larrea divaricata*) and white bursage (*Ambrosia deltoidea*) [8], although ironwood (*Olneya tesota*), palo verde (*Cercidium floridum*), Joshua tree (*Yucca brevifolia*), and ocotillo (*Fouquieria splendens*) are also found throughout the region.

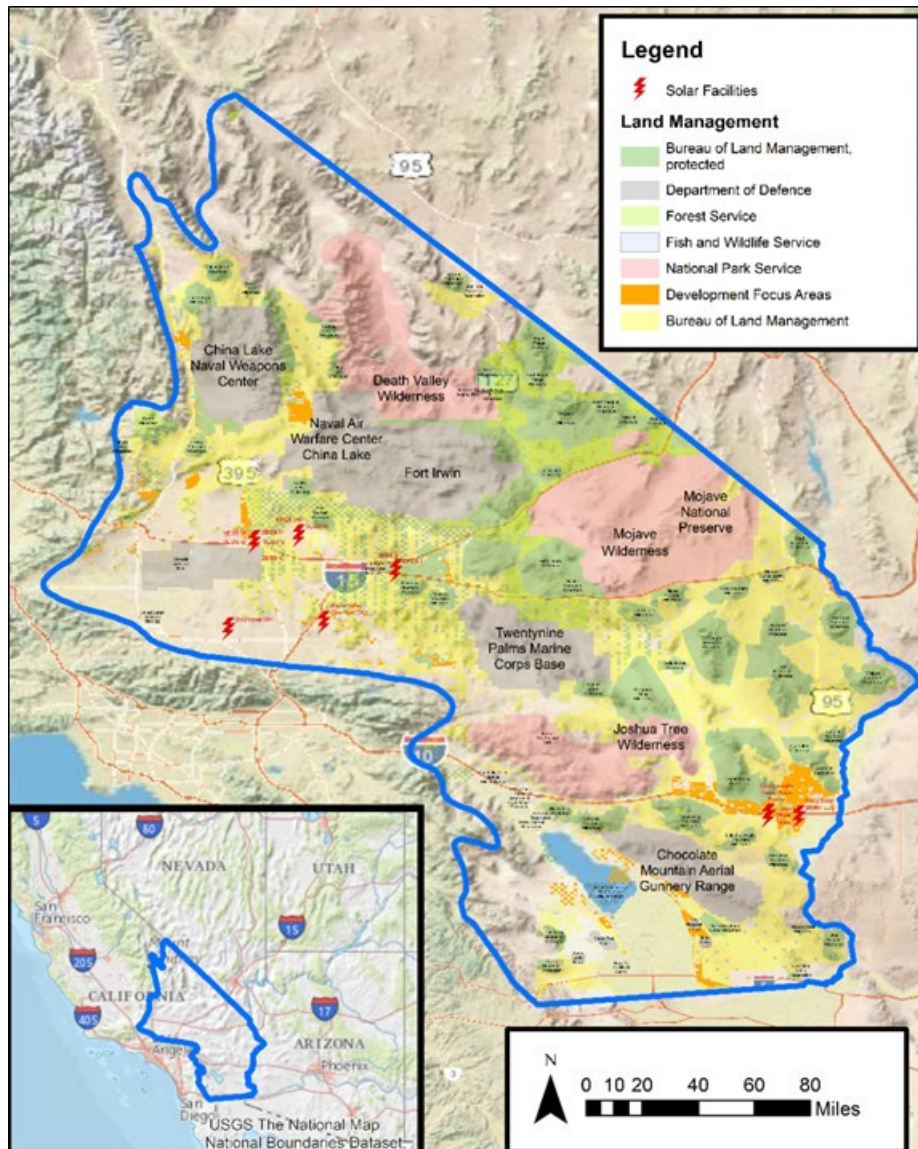


**Figure 1.** Map of the Desert Renewable Energy Conservation Plan (DRECP) study area in southern California showing boundaries of National Parks, BLM-protected Wilderness Study Areas (WSAs), and Development Focus Areas (DFAs) with solar energy development site names.

Dry lakes (also called playas) are unique geomorphic features in the DRECP study area (Table 1). Small playas may occur as irregularities in alluvial fans, separate from larger playas, in enclosed basins formed by faulting [11]. Desert playas may be periodically filled with surface water from runoff, direct precipitation, or groundwater discharge. Annual variation is such that a given playa may not become flooded at all during a relatively rainy year or remain flooded for up to three years [12].

**Table 1.** Largest dry lakes (playas) in the Mojave Desert region of California [11].

Playa Name	Area (km <sup>2</sup> )	Approximate Center Location
Rogers and Rosamond	97	34.83° N, 118.07° W
Owens Lake	448	35.50° N, 117.91° W
Death Valley–Badwater	96	36.25° N, 116.82° W
Panamint Valley	1680	36.10° N, 117.24° W
Bristol, Cadiz, and Danby	193	34.28° N, 115.38° W
Searles Lake	96	35.73° N, 117.30° W

Three National Parks (Death Valley, Mojave National Preserve, and Joshua Tree) occupy a sizable fraction of the DRECP study area, in addition to more than ten federally protected National Wilderness Areas (NWA) mainly under the management of the Bureau of Land Management (BLM). The coverage areas of five major military bases (China Lake, Fort Irwin, Edwards Air Force Base, Twenty-Nine Palms, and Chocolate Mountains Gunnery Range) are also shown in Figure 1.

The Antelope Valley groundwater basin [13] in the western Mojave Desert (Los Angeles County) is home to two of the largest cities in the study area, Palmdale and Lancaster. It is a triangular valley area, bounded on the southwest by the San Gabriel Mountains, on the northwest by the Tehachapi Mountains, and by ridges and buttes on the north and east sides. This valley has extensive dry lakes and internal drainage, with runoff from the surrounding mountains draining towards dry lakebeds in the lower parts of the valley. Land use in the valley is approximately 68% natural (mostly shrubland and grassland), 24% agricultural, and 8% urban [14]. Recharge to the groundwater system is primarily runoff from the surrounding mountains, and by direct infiltration of irrigation water and sewer systems. The primary sources of discharge are pumping from wells and evapotranspiration across the dry lakebeds [15].

Since the early 1970s, groundwater has provided between 50 and 90 percent of the total water supply in Antelope Valley. Over these past 50 years, groundwater pumping has resulted in water-level declines of more than 60 m (200 ft) in parts of the basin and land subsidence of more than 2 m (6 ft) in some areas [16]. Most of the land subsidence has occurred around the Rogers and Rosamond dry lakebeds just north of Lancaster [17].

### 3. Materials and Methods

#### 3.1. MODIS Land Surface Temperature Data

The Land Surface Temperature (LST) and emissivity 8-day composite data (MOD11A2) are retrieved at 1-km ground resolution by a generalized split-window algorithm [18], in which emissivities in MODIS bands 31 and 32 (covering wavelengths 10.78–11.28  $\mu\text{m}$  and 11.77–12.27  $\mu\text{m}$ , respectively) are estimated from land cover types, atmospheric column water vapor, and lower boundary air surface temperature separated into tractable sub-ranges for optimal retrieval [19]. In the day/night algorithm, daytime and nighttime LSTs (in kelvin) and surface emissivities are retrieved from pairs of day and night MODIS observations in seven thermal infrared (TIR) bands.

The complete (2000–2018) LST time series data layer was obtained using the “MODISTsp” R package download client [20]. We selected all LST layers for the study region of the original MODIS HDF files, plus additional quality indicators from aggregated MODIS quality assurance layers. Virtual files allowing access to the entire time series as a single file were also created.

Any pixel observations that had been contaminated with clouds, snow, or ice were eliminated from each dataset according to pixel reliability values. Each biweekly LST dataset was reaggregated to monthly observations based on the maximum reported value in a given month. Reaggregation was necessary to reduce processing time for subsequent steps. The maximum values were selected as the reaggregation statistic to further reduce any chance of atmospheric contamination, which would tend to decrease a given LST reading.

Any remaining missing data was only interpolated linearly if the time series did not have greater than 5% missing data or did not have four or more consecutive missing data points. The final result was a raster dataset for each LST containing 8-day composited observations from February 2000 to May 2018.

It should be noted that MOD11 LST products have shown a negative value bias of between 1° and 3° K over certain arid regions of China [21]. While newer MOD21 products are being evaluated to correct for such biases, these datasets are available for just a few years and are not mature beyond a provisional status. Moreover, even if MOD11 products have a consistent absolute bias of several degrees K over some arid regions, the relative time-series trends in MOD11 should still be the same as for any new MOD21 products.

### 3.2. Time Series Change Detection and Statistical Analyses

The BFAST models a time series according to the following general Algorithm:

$$Y(t) = S(t) + T(t) + e(t) \quad (1)$$

where  $t$  is time,  $Y(t)$  is the observed LST value of the time series,  $S(t)$  is the seasonal cycle,  $T(t)$  is the linear trend component, and  $e(t)$  is the residual error [22]. BFAST decomposes a time series into seasonal and linear trend components. By isolating the linear trend component from the seasonal signal, significant changes not attributable to seasonality may be identified from structural change tests. These breakpoints shifts (simply called “breakpoints” from here) are significant changes in the linear trend component of the model, and represent anomalous perturbations in a time series [22]. The ordinary least squares (OLS) residuals-based MOving SUM (MOSUM) was applied to test for one or more breakpoints occurring [9]. If the test indicated significant structural change ( $p < 0.01$ ), then break points were estimated.

BFAST methods were implemented by adapting an existing R package (“bfast”) to iterate over raster grids [22]. We obtained change detection results by running this BFAST for each LST dataset in the study areas. The BFAST model was parametrized to find a maximum of five breakpoints at a minimum time length of 11 months apart to capture only larger changes at an approximately yearly time scale. The significance level for structural change was set to  $p < 0.01$ .

### 3.3. Long-Term Climate Records

Two weather station locations that offered daily precipitation records since the early 1990s were selected for comparisons to MODIS LST changes across the study area. These stations were located near the cities of Victorville (34.47° N, 117.25° W; San Bernardino County) and Blythe (33.37° N, 114.36° W; Riverside County). The daily precipitation records since 1995 were downloaded from the Western Regional Climate Center ([wrcc.dri.edu](http://wrcc.dri.edu)).

## 4. Results

### 4.1. Breakpoint Patterns

Structural changes in the LST time series from BFAST analysis at four selected locations (Figure 2) were plotted to illustrate the differences between breakpoint patterns within dry lake beds, wildfire burn areas (according to Monitoring Trends in Burn Severity fire boundary records), and solar energy development locations. Both BFAST results for Rosamond Dry Lake and Death Valley Badwater Playa (Figure 2a,b, respectively) showed negative (abrupt cooling) breakpoints during the winter (coldest) periods of 2004 and 2005. BFAST results for the Covington Flats area in Joshua Tree National Park (Figure 2c) showed a positive (abrupt warming) breakpoint following the 2006 Whispering Pines Fire [23]. At the location of the McCoy I solar energy facility in the southern McCoy Mountain washes, the LST was unchanging between 2000 and 2014 (Figure 2d), but then decreased significantly after a breakpoint that was detected in 2015.

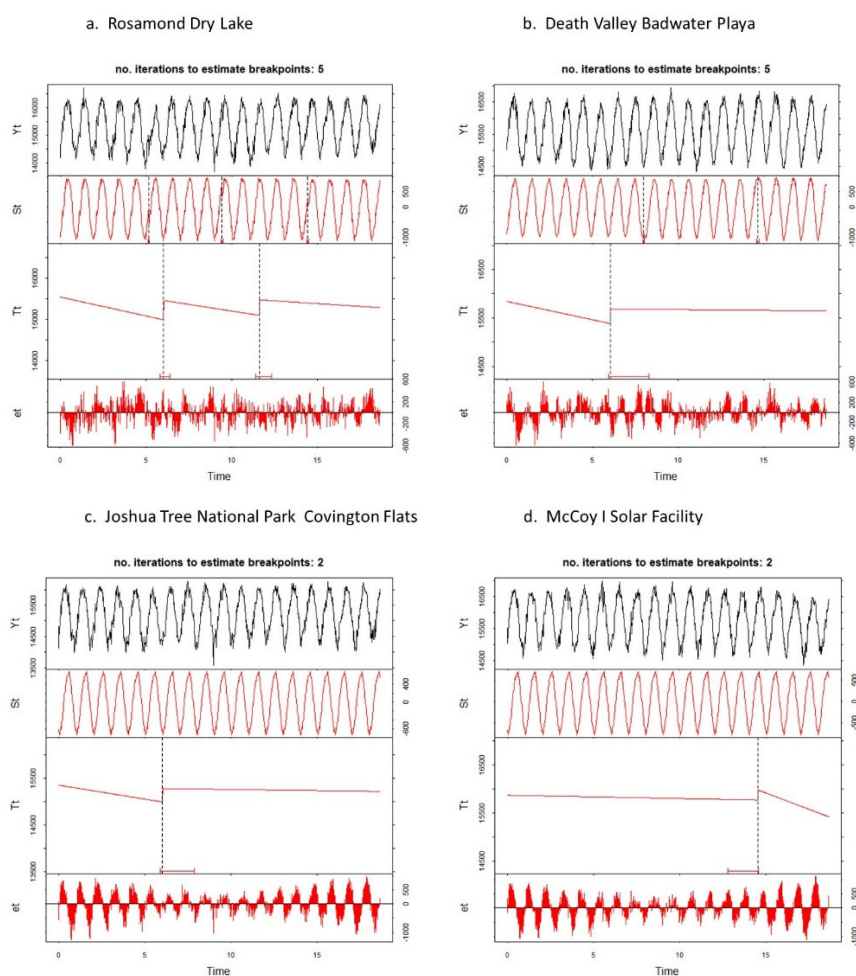


**Figure 2.** Breaks for Additive Seasonal and Trend (BFAST) output plots for four locations between 2000 and 2018 for the Moderate-Resolution Imaging Spectroradiometer (MODIS) land surface temperature (LST) 1-km monthly time series.  $Y(t)$  is the time-series of MODIS LST values;  $S(t)$  is the fitted seasonal component;  $T(t)$  is the fitted trend component;  $e(t)$  is the noise component; statistical breakpoints ( $p < 0.01$ ) are identified by vertical dashed lines. Year numbers on the horizontal axis start at 1 = 2000 and end in early 2018. (a) and (b) show two dry lakes, (c) shows a burned area in the National Park, and (d) shows a newly constructed solar energy facility.

BFAST results for the largest dry lakes within the study area (Table 1) were each mapped to examine the geographic details of breakpoint patterns (Figure 3). Results showed that all of these playas experienced multiple LST breakpoints since the year 2000. The central areas of these dry lakes responded with more than three breakpoints in all cases shown, indicating a repeated pattern of wetting and drying that controlled surface temperatures with abrupt negative (cooling) and positive (warming) cycles. The dates most common to these dry lake LST breakpoints were detected during 2004 and 2005.

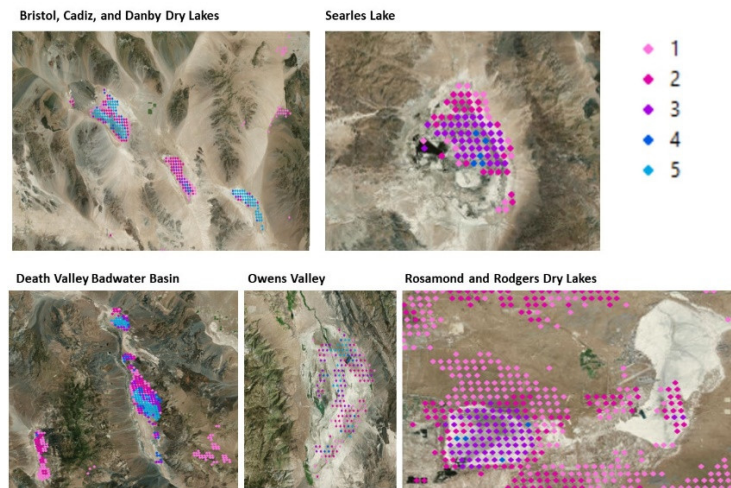


**Figure 3.** Breakpoints detected in selected dry lakes (as true-color images) within the study region from structural change analysis of LST between 2000 and 2018 for the MODIS 1-km monthly time series. Number of breakpoints per pixel shown in the color legend (upper right). All maps are upward in the northern direction.

According to the United States Forest Services mapping in the Monitoring Trends in Burn Severity (MTBS) program ([www.mtbs.gov](http://www.mtbs.gov); [23]), there were 51 large wildfires recorded within the DRECP study area between 2000 and 2015. About 40% of these burned areas were detected with at least one breakpoint during the year the fire broke out. All but one wildfire area showed a majority of positive (abrupt warming) LST breakpoints. An example of the LST breakpoint pattern detected within the 13,000 ha Powerhouse Fire (2013) boundary area near Antelope Valley confirmed the predominance of positive (abrupt warming) breakpoints following the date of the fire ignition (Figure 4), and the contrasting presence of negative (abrupt cooling) breakpoints in a lower-elevation protected State Parks reserve area just outside the burned area boundary.

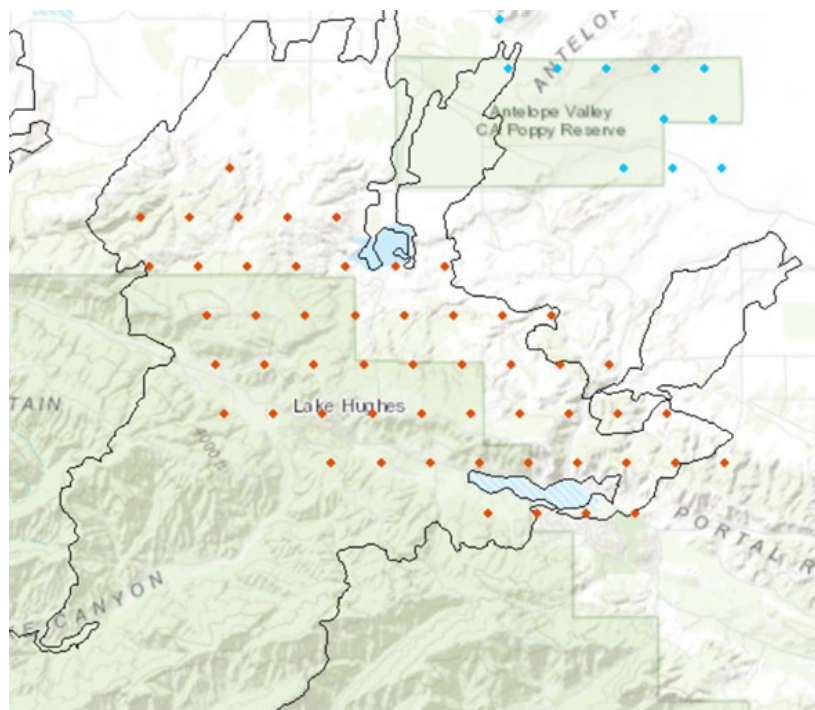


**Figure 4.** Boundary map of the Powerhouse Fire (2013; solid line) near Antelope Valley, CA, showing positive breakpoints (in orange) and showing negative breakpoints for 2013 (in blue). Map is upward in the northern direction.

4.2. Change Detection at Solar Energy Development Sites

Four solar energy facilities have been constructed in the Lower Colorado Desert over the past decade for which to examine the LST structural change results (Table 2). A negative (abrupt cooling) LST breakpoint of between 1.5 °C and 2.5 °C was detected by BFAST at each of these facility locations in the year or two following the reported start of construction (Figure 5). No LST breakpoints were detected on the sparsely vegetated desert surfaces immediately surrounding the energy facility sites.

Table 2. Construction start dates for solar energy sites.

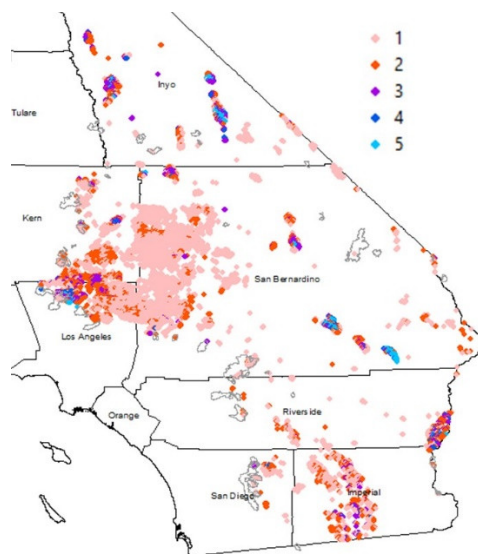
Site	Construction Start Date	Source
Desert Stateline	October 2014	Southern Power 2018
Desert Sunlight	September 2011	First Solar
Genesis	December 2010	National Renewable Energy Laboratory
McCoy I	September 2015	United State Energy Information Administration



Figure 5. Map of single breakpoints (shaded circle symbols) detected from structural change analysis of LST at solar energy construction facilities in the Lower Colorado Desert. All maps are upward in the northern direction.

4.3. Breakpoint Detection at the Regional Scale

BFAST analysis detected at least one LST breakpoint in about 8% of the 1-km cells, representing 9419 km<sup>2</sup> within the DRECP study area (Figure 6). Area-wide results showed five times more positive LST breakpoints (abrupt temperature warming events) than negative breakpoints (Figure 7). Locations that showed more than one breakpoint over the 18-year LST time series comprised about 2.5% of the entire study area, evenly divided between positive and negative breakpoints.



**Figure 6.** Map of breakpoints detected from structural change analysis of LST between 2000 and 2018 for MODIS 1-km monthly time series. All Monitoring Trends in Burn Severity (MTBS) wildfire boundaries since the year 2000 are shown as gray outlines. Number of breakpoints per pixel shown in the color legend (upper right).

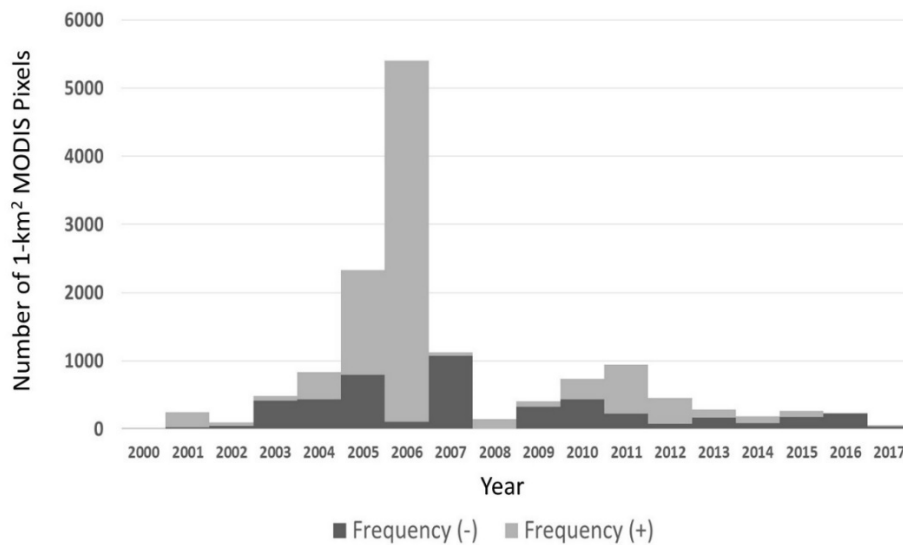


**Figure 7.** Yearly distribution of positive (warming) and negative (cooling) breakpoints detected from structural change analysis of LST of the DRECP study area between 2000 and 2018 for the MODIS 1-km monthly time series.

The year detected with the most LST breakpoints was 2006, whereas the year with the fewest LST breakpoints was 2017. The year with the highest number of negative (abrupt cooling) LST breakpoints was 2007. Over the entire time series, the month of the year detected with the most LST breakpoints (both positive and negative) was March, whereas the month with the fewest LST breakpoints was August (Figure 8). The monthly distribution of breakpoints detected from an example year of 2005 showed that negative (abrupt cooling) events occurred overwhelmingly in the months of January and February, whereas positive (abrupt warming) events occurred overwhelmingly in the months of April and October (Figure 9).

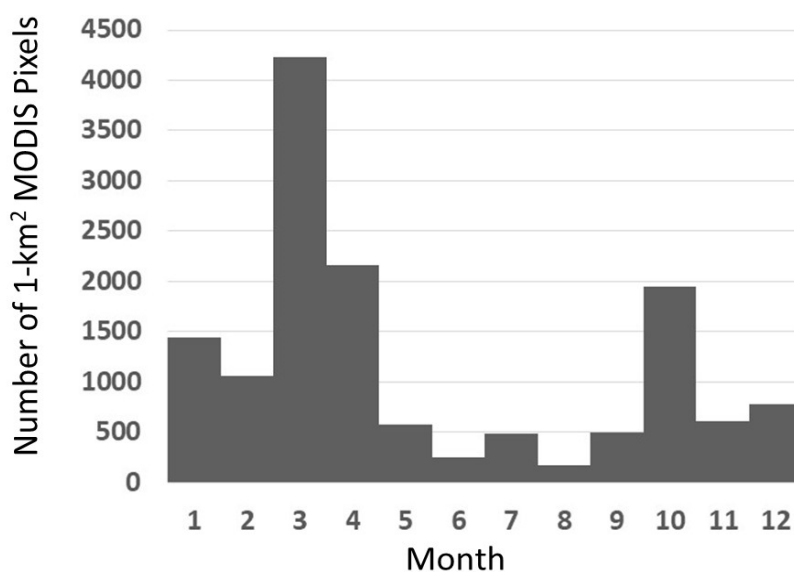


**Figure 8.** Monthly distribution of all breakpoints detected from structural change analysis of LST of the DRECP study area between 2000 and 2018 for the MODIS 1-km time series.

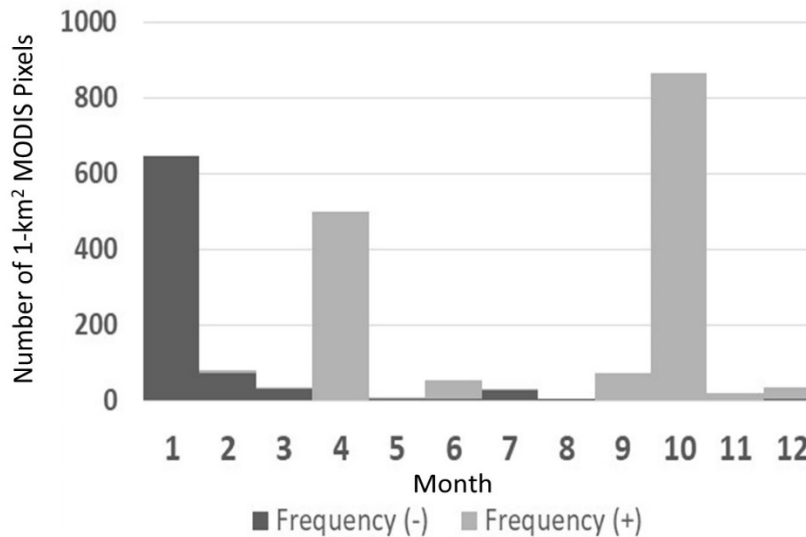


**Figure 9.** Monthly distribution of negative and positive breakpoints detected from structural change analysis of LST in 2005 for the DRECP study area MODIS 1-km time series.

The majority of LST breakpoints in the DRECP cover region were clustered in Antelope Valley and Edwards Air Force Base areas (centered around 34.83° N, 118.08° W), which has been urbanized widely and developed for military bases over past decades. About 54% of the LST breakpoints in Antelope Valley were detected in the year 2005 and 30% in 2004 on landforms that can be described generally as playas and subsided sub-basins. More than 70% of these were positive (abrupt warming) breakpoints and less than 30% were detected as negative (abrupt cooling) breakpoints.

4.4. Association of Breakpoint Dates with Precipitation Events

The year detected with the most LST breakpoints, 2006, was preceded by the consistently rainiest winter season in the long-term precipitation record for two weather station locations that spanned the study area (shown in Figure 10). The annual rainfall total for 2005 at Victorville was 227 mm, which was second only to 2010 with 364 mm. The annual rainfall total for 2005 at Blythe was 163 mm, which was second only to 1998 with 163 mm. The daily totals of rainfall detected with the fewest LST breakpoints, i.e., during 2017, were preceded by six consecutive years of extremely low rainfall totals across the study region, at less than 125 mm per year at both weather station locations (Figure 10).

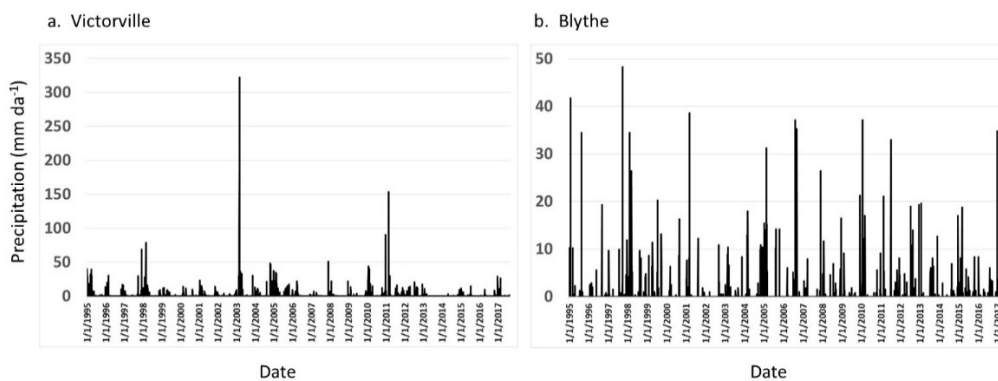


**Figure 10.** Daily precipitation records for two weather station locations within the study area. Note that the vertical axes have different ranges of precipitation values.

#### 4.5. Surface Temperature Trends at the Regional Scale

Over the majority of the study area, BFAST results showed positive (warming) LST trends between the years 2000 and 2018 (Figure 11). Among pixels with no breakpoints detected, both LST trends were skewed toward positive slope (warming) values (Figure 12). The western-most margins of the study area showed consistent widespread warming trends, whereas the eastern portions of the Mojave and Lower Colorado Deserts showed a mix of positive and neutral LST trends. Long-term negative (cooling) LST trends were detected only in relatively small portions of some of the largest dry lake formations in the Antelope Valley, Death Valley, and Bristol, Cadiz, and Danby playas (Figure 11).

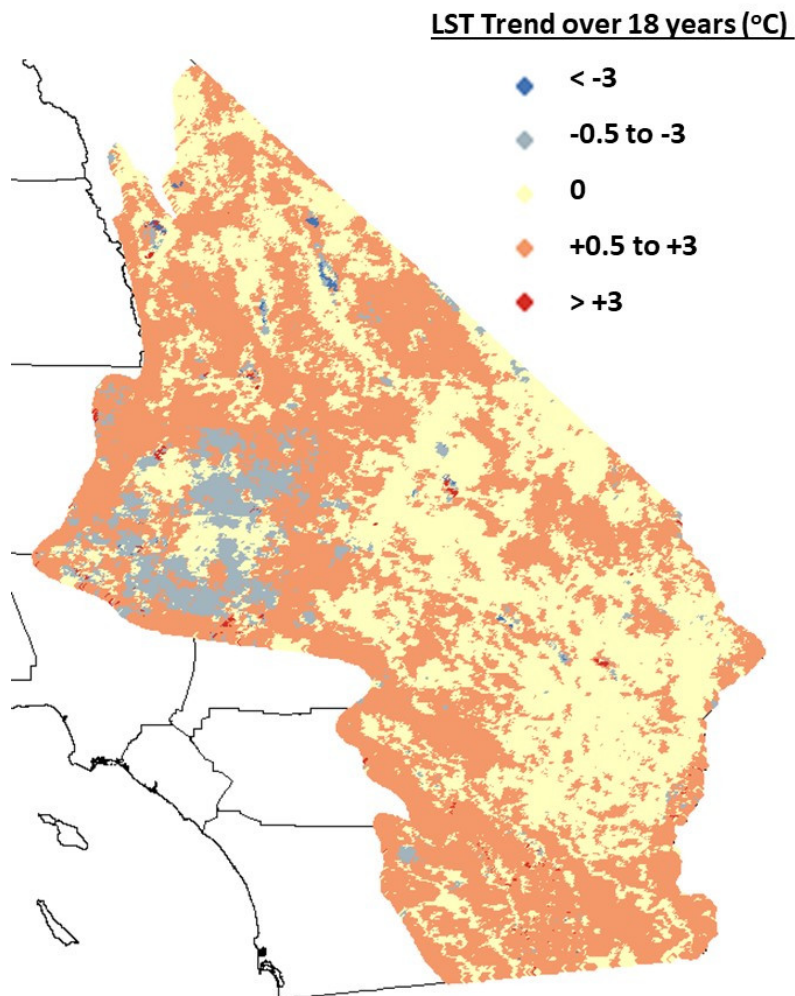


**Figure 11.** Map of slope trends detected from structural change analysis of LST between 2000 and 2018 for MODIS 1-km monthly time series. Positive (warming) LST slope values in orange-red shades and negative (cooling) LST slope values in blue shades; areas of no change in LST are shaded in yellow.

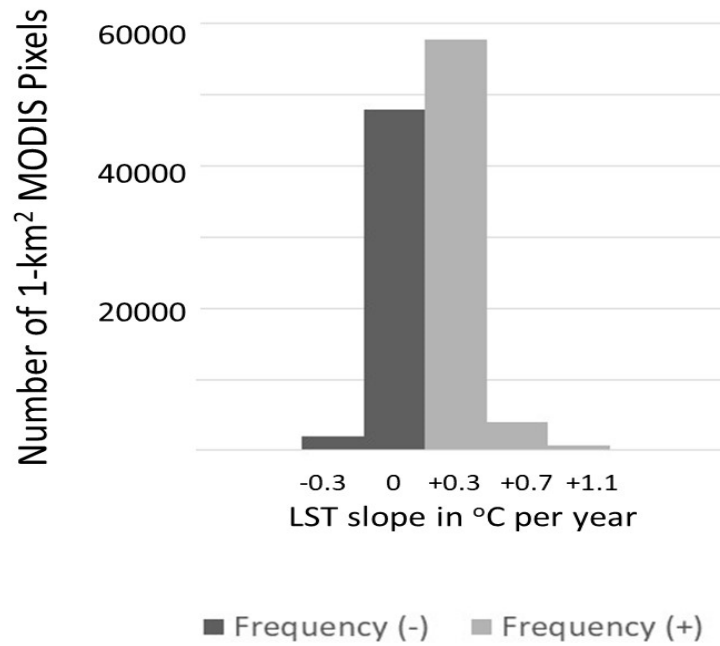


**Figure 12.** Distribution of LST slopes for all pixels with zero breakpoints detected from BFAST analysis in the DRECP study area between 2000 and 2018 for the MODIS 1-km time series.

A closer examination of 18-year LST trends on mountain-top ridges versus rocky slopes and playas of the eastern portions of the Mojave and Lower Colorado Deserts revealed a consistently varying landscape pattern of the highest warming trends in low-elevation sandy washes and playas, strong cooling trends on mid-elevation rocky slopes, and minimal change in LST over the time period on mountain-top ridges (Figures 13 and 14), except where fires have removed the shrub vegetation cover and exposed the soils beneath to gradual surface warming.

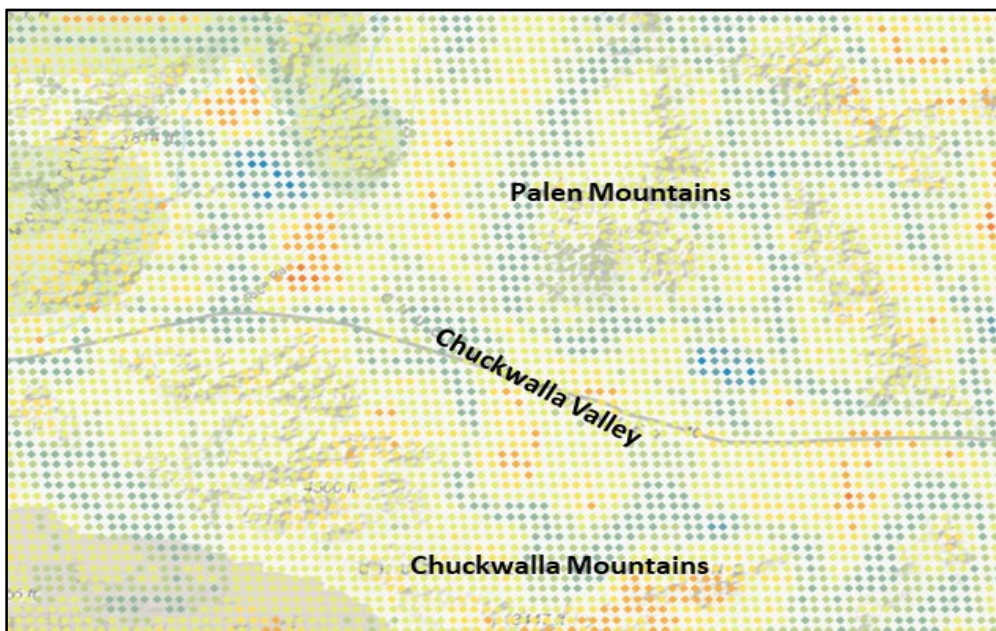


**Figure 13.** LST slope results for the Chuckwalla Valley and Palen-McCoy Wilderness in Riverside County, CA, with positive (warming) BFAST LST slope values in orange-red shades and negative (cooling) LST slope values in blue shades; areas of no change in LST are shaded in yellow. The map is upward in the northern direction.

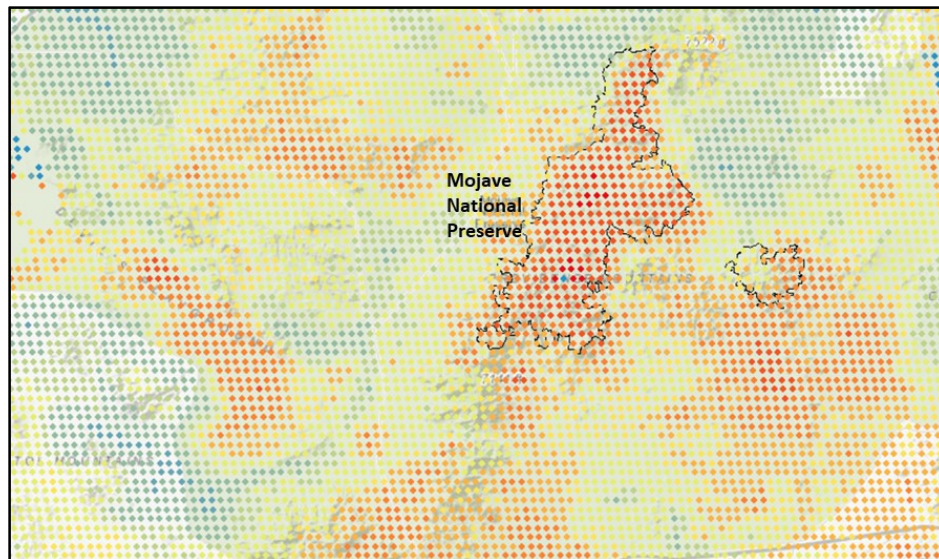


**Figure 14.** LST slope results around an area burned by the Hackberry Complex Fire of 2005 (centered at  $35.14^{\circ}$  N,  $115.41^{\circ}$  W) within the Providence Mountains of the Mojave National Preserve with positive (warming) BFAST LST slope values in orange-red shades and negative (cooling) LST slope values in blue shades; areas of change in LST are shaded in yellow. The map is upward in the northern direction.

The large agricultural growing areas of the Imperial Valley and surrounding the town of Blythe (in eastern Riverside County) have shown strong warming trends overall in LST during the 18-year period of MODIS data analysis (Figure 15). There were commonly multiple LST breakpoints (creating multiple slope lines) detected in the major growing valleys within the study areas (Figure 6), which made the results for a long-term trend detection more complicated and irregular to interpret than for non-agricultural areas that showed zero or one LST breakpoint detected. Variable yearly crop planting and harvest schedules can play a role in generating this type of high breakpoint frequency and diversity.

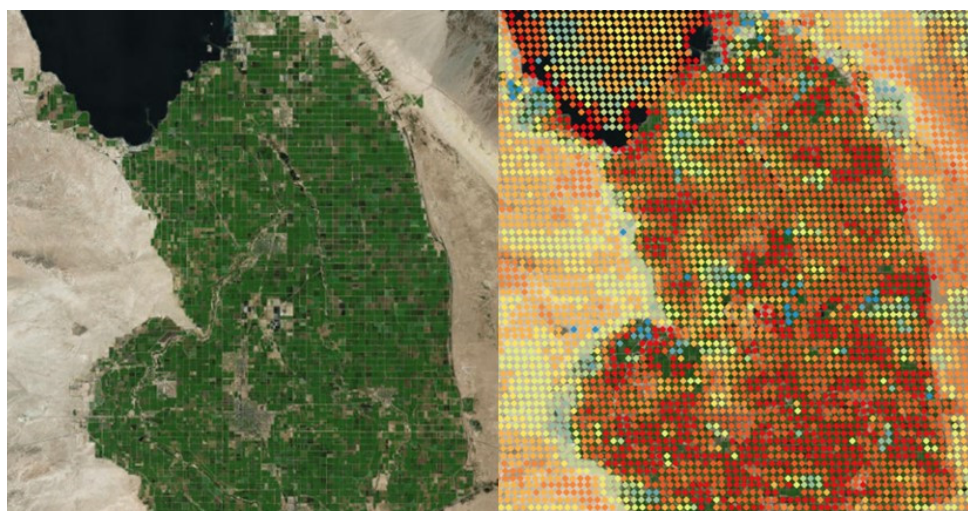


**Figure 15.** True color image (left panel) of the Imperial Valley cropland area, with positive BFAST LST slope values in orange-red shades and negative LST slope values in blue shades (right panel); no change in LST pixels are shaded in yellow. The map is upward in the northern direction.

## 5. Discussion

This BFAST change detection analysis for MODIS LST data sets collected over 18 years showed that negative (abrupt cooling) breakpoints are commonly associated with larger than average rainfall

periods, especially in dry lake playas of the Mojave Desert. BFAST results presented for Rosamond Dry Lake and Death Valley Badwater Playa as examples showed significant negative (abrupt cooling) breakpoints during the winter periods of 2004 and 2005, during what has been recorded as one of the consistently rainiest seasons in the long-term precipitation record for two weather station locations that spanned the study area. This timing of most LST breakpoints detected was observed over the entire study area as well. In the months following the surface cooling breakpoints at several Mojave Desert playa sites, LST started to increase again at a rate that could generate a follow-on positive (abrupt warming) LST breakpoint at the location, if local air temperatures are conducive to rapid surface drying and evaporation.

Dry lakes and playas in the Mojave Desert are among the lowest-elevation sites in the region and collect water only during periods when there is sufficient surface runoff, have no outlet, and lose all their water to evaporation [24]. In dry playas, ground water does not interact with the surface because the water table lies far below, typically >5 m deep. As a corroborating case study to our BFAST results, Reynolds et al. [25] reported that the eastern margin of Soda Lake (on the northern Carrizo Plain in San Luis Obispo County) has deep ground water levels where the playa sediments are hard packed and lack efflorescent salt. These authors reported that intensive precipitation events can result in flooding and standing water on surface of Soda Lake. Ground truth measurements and satellite imagery were able to document flooding events during the periods of both August 2003 and January–February 2005. Nine days after this playa flooded in January 2005, efflorescent salt could be observed as crystallized across the playa. The entire playa surface was deflated soon afterwards during a windstorm.

The uncommon abundance of dry lake beds and subsiding soils are the most plausible explanation for the high density of LST breakpoints detected in the Antelope Valley compared to any other sub-section of the study area. These dry playas in Antelope Valley were not found to have experienced strong LST warming trends over the 18-year study period like much of the rest of the western Mojave, but instead are subjected to regular negative (abrupt cooling) breakpoints that can dampen surface heating trends.

The southern California region frequently experiences temperature inversions, in which a layer of dry, warm air overlaying cool, moist air from the marine layer, is a common condition in the area. The cooler marine air capped by coastal clouds can be heavier than the warm air that acts as a top, through which the marine layer cannot pass. The Antelope Valley in particular does not frequently experience summer inversions that can “cap” low-elevation air layers in basin, although inversions can form during colder periods in the night time, then dissipating during daytime heating.

The detection of predominantly positive (abrupt warming) breakpoints following the date of fire ignitions throughout the study period suggested that the loss of live vegetation biomass in the Mojave Desert elevates the LST of comparatively barren land in post-fire years. Previous studies have corroborated the finding that burned areas in semi-arid ecosystems undergo a significant increase in LST after fire, which can be explained by the lower emissivity of combusted woody materials and changes in the energy balance related to vegetation removal [26,27]. Due to the scarcity of surface moisture in the desert environment, slow regrowth of shrub cover can produce warming trends that last for more than a few years after high-severity wildfires.

The repeated pattern across the study area of 18-year LST warming trends dominating low-elevation sandy washes and playas, strong cooling trends prevailing on mid-elevation rocky slopes, and minimal change in LST on mountain-top ridges has not been reported previously in published studies. This BFAST result leads us to hypothesize that the barren, rough and irregular rock surfaces with abundant shadows on mid-elevation slopes in the desert mountains do not absorb and re-radiate as much incident solar radiation (as do the relatively flat playa washes) and therefore are not warming over time in the same manner as the rest of the study region in southern California.

The BFAST result of negative (abrupt cooling) LST breakpoints of between 1.5 °C and 2.5 °C, coinciding with the dates of construction of solar energy facility locations in the Lower Colorado Desert, has been reported for the first time in the present study. Because no LST breakpoints were detected on the sparsely vegetated desert surfaces immediately surrounding these solar facility sites,

we conclude that the surfaces of energy producing materials have created new, relatively cool environments and habitats for the desert biota. The long-term impacts of these cooling habitats should be the subject of future field studies of plants and animal population changes around solar energy facilities.

## 6. Conclusions

Continuous monitoring and analysis of change in LST, together with other ecological variables, will be beneficial to conservation planning for biological populations across the desert region. Across the study area, positive LST breakpoints (abrupt temperature warming events) were five times more common than negative LST (surface cooling) breakpoints. The results of our 18-year time series of MODIS data showed strong surface warming trends across the western-most margins of the study area, whereas the eastern portions of the Mojave and Lower Colorado Deserts showed a mix of positive and neutral LST trends, strongly influenced by the complex topography of rocky mountain ranges. Long-term surface cooling trends were detected mainly in the largest dry lake formations in the Antelope Valley, Death Valley, and Bristol, Cadiz, and Danby playas. At several Mojave Desert playa sites, LST recovered from flooding and cooling events at rates that could generate a follow-on positive (abrupt warming) LST breakpoint. The implications of pervasive surface warming trends in the deserts of southern California are worthy of continued field monitoring to track the impacts of extreme heatwaves that could alter many ecological relationships in years to come.

**Author Contributions:** All authors have contributed equally to conceptualization, analysis, writing, and investigations.

**Funding:** This research was funded by the USA Department of the Interior Bureau of Land Management (BLM).

**Acknowledgments:** The authors wish to thank James Weigand of the BLM Field Office for comments on the study design. We are grateful to NASA for processing and providing MOD11 data sets, and to the Western Regional Climate Center for offering the climate data used in this study.

**Conflicts of Interest:** The authors declare no conflict of interest.

## References

1. Paul, E.A.; Clark, F.E. *Soil Microbiology and Biochemistry*; Academic Press: Cambridge, MA, USA, 1996; pp. 12–32.
2. Lehnert, M. Factors affecting soil temperature as limits of spatial interpretation and simulation of soil temperature. *Acta Univ. Palacki. Olomuc. Geogr.* **2015**, *45*, 5–21.
3. Potter, C.S. Landsat time series analysis of vegetation changes in solar energy development areas of the Lower Colorado Desert, Southern California. *J. Geosci. Environ. Prot.* **2016**, *4*, 1–6.
4. DRECP. Desert Renewable Energy Conservation Plan Homepage. 2018. Available online: <https://www.drecp.org> (accessed on 1 August 2018).
5. Li, Z.; Guo, X.; Dixon, P.; He, Y. Applicability of Land Surface Temperature (LST) estimates from AVHRR satellite image composites in northern Canada. *Prairie Perspect.* **2008**, *11*, 119–130.
6. Quan, J.; Zhan, W.; Chen, Y.; Wang, M.; Wang, J. Time series decomposition of remotely sensed land surface temperature and investigation of trends and seasonal variations in surface urban heat islands. *J. Geophys. Res. Atmos.* **2016**, *121*, 2638–2657.
7. Zhan, W.; Huang, F.; Quan, J.; Zhu, X.; Gao, L.; Zhou, J.; Ju, W. Disaggregation of remotely sensed land surface temperature: A new dynamic methodology. *J. Geophys. Res. Atmos.* **2016**, *121*, 10538–10554.
8. Coppernoll-Houston, D.; Potter, C.S. Field measurements and satellite remote sensing of daily soil surface temperature variations in the Lower Colorado Desert of California. *Climate* **2018**, *6*, 94, doi:10.3390/cli6040094.
9. Verbesselt, J.; Hyndman, R.; Newnham, G.; Culvenor, D. Detecting trend and seasonal changes in satellite image time series. *Remote Sens. Environ.* **2010**, *114*, 106–115.
10. Marks, J.B. Vegetation and soil relations in the Lower Colorado Desert. *Ecology* **1950**, *31*, 176–193.
11. McNab, W.H.; Avers, P.E. (Eds.) *Ecological Subregions of the United States: Section Descriptions*; WO-WSA-5; USDA Forest Service, Ecosystem Management: Washington, DC, USA, 1994.

12. Brostoff, W.; Lichvar, R.; Sprecher, S. *Delineating Playas in the Arid Southwest: A Literature Review*; Technical Report ERDC TR-01-4; US Army Corps of Engineers, Engineer Research and Development Center: Fort Belvoir, VA, USA; 2011; 34p.
13. Cooke, R.; Warren, A.; Goudie, A. *Desert Geomorphology*; UCL Press: London, UK, 1993.
14. California Department of Water Resources. California's Groundwater: California Department of Water Resources Bulletin 118. 2003. 246p. Available online: [www.water.ca.gov/groundwater/bulletin118/update2003.cfm/](http://www.water.ca.gov/groundwater/bulletin118/update2003.cfm/) (accessed on November 1, 2018).
15. Schmitt, S.J.; Milby Dawson, B.J.; Belitz, K. Groundwater Quality Data in the Antelope Valley Study Unit, 2008—Results from the California GAMA Program: U.S. Geological Survey Data Series 479. 2009. 79p. Available online: [pubs.usgs.gov/ds/479/](http://pubs.usgs.gov/ds/479/) (accessed on November 1, 2018).
16. Siade, A.J.; Nishikawa, T.; Rewis, D.L.; Martin, P.; Phillips, S.P. *Groundwater Flow and Land Subsidence Model of Antelope Valley*; Scientific Investigations Report 2014-5166; U.S. Geological Survey: Menlo Park, CA, USA, 2014; p. 136.
17. Galloway, D.; Hudnut, K.; Ingebritsen, S.; Phillips, S.; Peltzer, G.; Rogez, F.; Rosen, P. Detection of aquifer system compaction and land subsidence using interferometric synthetic aperture radar, Antelope Valley, Mojave Desert, California. *Water Resour. Res.* **1998**, *34*, doi:10.1029/98WR01285.
18. Wan, Z.; Dozier, J. A generalized split-window algorithm for retrieving land-surface temperature from space. *IEEE Trans. Geosci. Remote Sens.* **1996**, *34*, 892–905.
19. Wan, Z.; Zhang, Y.; Zhang, Q.; Li, Z.-L. Validation of the land-surface temperature products retrieved from Terra Moderate Resolution Imaging Spectroradiometer data. *Remote Sens. Environ.* **2002**, *83*, 163–180.
20. Busetto, L.; Ranghetti, L. MODISstsp: An R Package for Automatic Preprocessing of MODIS Land Products Time Series. *Comput. Geosci.* **2016**, *97*, 40–48, doi:10.1016/j.cageo.2016.08.020.
21. Hua, L.; Sun, D.; Yu, Y.; Wang, H.; Liu, Y.; Liu, Q.; Du, Y.; Wang, H.; Cao, B. Evaluation of the VIIRS and MODIS LST products in an arid area of Northwest China. *Remote Sens. Environ.* **2014**, *142*, 111–121.
22. Zeileis, A. A unified approach to structural change tests based on ML scores, F statistics, and OLS residuals. *Econom. Rev.* **2005**, *24*, 445–466.
23. Eidenshink, J.; Schwind, B.; Brewer, K.; Zhu, Z.; Quayle, B.; Howard, S. A project for monitoring trends in burn severity. *Fire Ecol. Spec. Issue* **2007**, *3*, 3–21.
24. Mojave Integrated Regional Water Management Plan (IRWMP). *Kennedy-Jenks Consultants*; K/J Project No. 1389002; IRWMP: Oxnard, CA, USA, 2014; 400p.
25. Reynolds, R.L.; Yount, J.C.; Reheis, M.; Goldstein, H.; Chavez, P., Jr.; Fulton, R.; Whitney, J.; Fuller, C.; Forester, R.M. Dust emission from wet and dry playas in the Mojave Desert, USA. *Earth Surf. Process. Landf.* **2007**, *32*, 1811–1827.
26. Vlassova, L.; Pérez-Cabello, F.; Rodrigues, M.; Montorio, R.; García-Martín, A. Analysis of the relationship between land surface temperature and wildfire severity in a series of Landsat images. *Remote Sens.* **2014**, *6*, 6136–6162.
27. Veraverbeke, S.; Verstraeten, W.W.; Lhermitte, S.; Van De Kerchove, R.; Goossens, R. Assessment of post-fire changes in land surface temperature and surface albedo, and their relation with fire-burn severity using multitemporal MODIS imagery. *Int. J. Wildl. Fire* **2012**, *21*, 243–256.

